

Extended Task and Motion Planning of Long-horizon Robot Manipulation

Tianyu Ren*, Georgia Chalvatzaki*, and Jan Peters*

*Computer Science Department, Technische Universität Darmstadt

Abstract—Task and Motion Planning (TAMP) requires the integration of symbolic reasoning with metric motion planning that accounts for the robot’s actions’ geometric feasibility. This hierarchical structure inevitably prevents the symbolic planners from accessing the environment’s low-level geometric description, vital to the problem’s solution. Most TAMP approaches fail to provide feasible solutions when there is missing knowledge about the environment at the symbolic level. The incapability of devising alternative high-level plans leads existing planners to a dead end. We propose a novel approach for decision-making on extended decision spaces over plan skeletons and action parameters. We integrate top-k planning for constructing an explicit skeleton space, where a skeleton planner generates a variety of candidate skeleton plans. Moreover, we effectively combine this skeleton space with the resultant motion parameter spaces into a single *extended* decision space. Accordingly, we use Monte-Carlo Tree Search (MCTS) to ensure an exploration-exploitation balance at each decision node and optimize globally to produce minimum-cost solutions. The proposed seamless combination of symbolic top-k planning with streams, with the proved optimality of MCTS, leads to a powerful planning algorithm that can handle the combinatorial complexity of long-horizon manipulation tasks. We empirically evaluate our proposed algorithm in challenging manipulation tasks with different domains that require multi-stage decisions and show how our method can overcome dead-ends through its effective alternate plans compared to its most competitive baseline method.

I. INTRODUCTION

The intelligent robots of the future should perform multiple tasks in unstructured environments, like houses, hospitals, etc. Among the most critical features in robotics is the need for reasoning and acting for achieving multi-stage long-horizon tasks that require manipulation and mobility. Traditional approaches considered long-horizon manipulation as a strict decomposition of sub-tasks, either hard-coded or addressed as individual sub-problems to be solved independently. Inspired by advances in symbolic *Artificial Intelligence (AI) planning*, the previous strict hierarchical approach is now getting automated by a single solution for *Task and Motion Planning (TAMP)* [1, 2]. With a typical TAMP solver, in the high level, a task planner reasons over a sequence of symbolic actions for reaching a symbolic goal state; in the low level, a set of motion planners search for metric decisions to make each action geometrically feasible w.r.t. the environment.

TAMP hierarchical structure makes it suitable for solving long-horizon tasks; however, it brings some major issues in coordinating the two levels of symbolic reasoning and geometric planning. Since the task planner is mostly uninformed about detailed constraints of the environment, it tends to generate

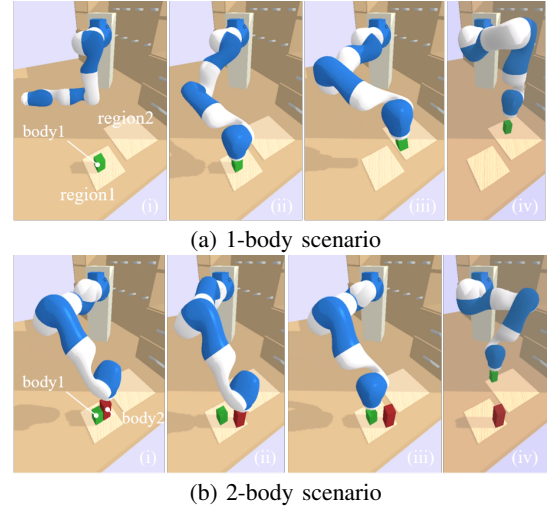


Fig. 1: Example task: transportation of body1 from region1 to region2. Bodies can only be grasped from the top. Though the 1-body scenario is trivial to most TAMP algorithms, the 2-body scenario is more challenging: the taller red body must be relocated before the green one can be reached without collisions.

symbolic plans that are geometrically infeasible. Most TAMP algorithms start with only one symbolic plan that is considered “optimal”. Sometimes such a plan may be enough (Fig. 1a). However, in more challenging scenarios, e.g., Fig. 1b, this single plan fails quickly. This issue is commonly described as an *incomplete domain description* [3, 4] in the sense that the task planner does not have enough domain knowledge to generate absolutely correct results.

Like AI planning, TAMP is an intrinsic offline process that relies heavily on the associated domain description. Research has delivered significant advancements, especially with the introduction of integrated TAMP methods [1, 2, 5, 6, 7], however particular domain specifications and assumptions hinder their application in real-world settings. Some of the common assumptions in TAMP approaches [7] consider that the environment is fully known to the task planners, objects and robots are rigid-bodies with known kinematics, the actions in the world are deterministic, etc. Although there are domains where detailed knowledge engineering is necessary and feasible, e.g., mission planning in spacecrafts, this is inapplicable to most real-world scenarios [8]. Over-engineered domains do not allow the planner to generalize across different environments, robots, etc. A key requirement for efficient robotic TAMP is *generality* through the generation of alternate task plans independent of particular domain specifications.

This paper proposes a novel framework for general-purpose TAMP with extended decision spaces (eTAMP). Our proposed method generates diverse alternate symbolic plans (skeletons) for an extended decision space, optimizing both the skeleton selection and the actions' parameters' concrete bindings. We propose using a top-k skeleton planner to produce diverse skeletons, guaranteeing that no better solution exists under a current domain description [9]. Moreover, we augment the skeleton planner with streams [6, 10], a sampling procedure that uses black-box conditional generators of action parameters in the task planning domain, as additional operators for symbolic AI planning. Streams address the hybrid discrete-continuous planning domains like those in PDDLStream [10, 6]. We integrate the decision over skeletons as an "additional stream" for sampling alternate skeletons in the TAMP's symbolic subspace. Notably, we propose using Monte-Carlo Tree Search (MCTS) to solve this stochastic decision-making problem over skeletons and concrete bindings of the action parameters. The main contribution of this work is twofold:

- we reformulate the TAMP framework by transforming the problem of skeleton planning with incomplete domain description into a series of generic planning problems that are tractable to any off-the-shelf top-k planner;
- we propose a tree-structured search algorithm for solving the resultant stochastic decision-making problem in the extended decision space.

We evaluate our proposed framework on challenging robotic tasks defined in various domains and long-horizon tasks with increasing difficulty, using both a 7-degrees-of-freedom (dof) manipulator and a 10-dof mobile manipulator robot. Our empirical results prove the ability of the proposed eTAMP method to find feasible plans in challenging manipulation scenarios by producing alternate skeletons and the decision of motion parameters of the actions compared to the state-of-the-art, thus taking one more step towards the creation of general-purpose robotic TAMPs.

II. RELATED WORK

Incomplete domain specification is ubiquitous in TAMP applications. This incomplete domain fails to capture several environmental constraints crucial to the feasibility of the generated skeletons. A robust TAMP algorithm should search for alternate skeletons. Recent methods can discover new skeletons using replanning or reattempting mechanisms [10, 6, 11], and those are, in the best case, patched versions of the original infeasible plans. Therefore, most of the space of alternate skeletons will remain unexplored.

In particular, for robot TAMP, the developed algorithmic solutions vouched for performance instead of completeness and generality of the proposed planners [5]. A comprehensive review over integrated TAMP approaches can be found in [7]. Research for TAMP has been frequently approached as an optimization problem using logic geometric programming [12], or multi-modal motion planning with motion-modes switches for various tasks [13]. However, these methods are

designed for particular manipulation problems and are not applicable across different domains.

We are concerned with TAMP problem formulations that use the Planning Domain Definition Language (PDDL) [14] for the task domain description. PDDL is used to symbolize the original planning domain to individual actions with pre-conditions and effects. Early works for TAMP used semantic attachments in PDDL for querying motion planners over the feasibility of task actions [15]. However, this method requires a pre-specification of sets of discrete parameters like object poses, grasps, and robot configurations. Several methods consider finding constraint-satisfying states as in [5] to search for feasible task plans given some geometric constraints. [16] directly samples feasible regions for actions using conditional samplers.

The need for alternate skeletons remains an open research problem for generalization over different domains. Notably, in [11] the authors try to explicitly generate alternate skeletons through incremental solving. If the motion planner fails to refine a skeleton, they add additional feasibility constraints to the task planner. Similarly, in [2], the authors use an interface layer that generates logical facts that capture the failure of current skeletons and update the high-level state description. This heuristic treatment makes this decision process highly sub-optimal for new domains, ending up performing similarly to reattempting methods.

The robustness of TAMP and the quality of its solution will be improved by an extended optimal search in the skeleton space in addition to the search in the action parameter space. Top-k planning is one way of obtaining such a set, by finding a group of diverse solutions of size k . With a variety of candidate skeletons, it is possible to make a detour to avoid infeasible selections. Based on a Fast Downward [17, 18], [19] presents a complete top-k planner, the SYM-K, that scales efficiently to large sizes of k .

For searching for concrete bindings in a given decision space, MCTS methods (see App. VIII), such as UCT [20, 21], provides a probabilistically optimal solution by performing a sample-based tree search. [22] uses Voronoi partitioning with MCTS for achieving higher efficiency in robot planning, however, it is restricted to deterministic planning problems and therefore are not applicable to TAMP problems with stochastic transition functions.

In this work, we build on current advances in TAMP and symbolic top-k planning. We propose the use of PDDLstream that considers the metric sampling of the parameters of member actions, together with symbolic top-k planning for generating k candidate skeletons. Moreover, we propose the use of UCT on top of this extended decision space, for the designed algorithm to be used as general-purpose TAMP solver across different domains.

III. PRELIMINARIES

Robotic motion planning and AI planning. Motion planning demands a continuous *state-space formulation*, and sample-based methods have satisfactorily solved it (e.g., the rapidly

exploring dense tree family [23, 24]). Within AI planning, *logic-based formulations* (e.g., STRIPS and PDDL) have been conveniently used to compactly represent enormous discrete state spaces and produce outputs that logically explain the steps involved in arriving at some goal state. Several efficient searching heuristics (e.g., fast-forward [25], and fast-downward [17]) are specially proposed to adapt this logic-based formulation.

PDDL is an attempt to make AI planning modules more reusable, and easily comparable [26]. The three most important components of PDDL are the sets of *objects*, *predicates*, and *actions*. (i) Objects characterize the complete set of distinct existences in the world, for example, graspable bodies, placement regions, or motion trajectories that a robot can follow. (ii) A predicate is a Boolean function describing what combinations of arguments can be true. For example, a predicate "On(*?body*, *?region*)" is to determine if *?body* is placed on *?region*. When applied to specific set of objects, e.g., On(body1, region2), it indicates the fact that body1 is placed on region2 and it is now called a *literal*. (iii) An action changes the world state. For each *action* to be applicable, a set of *preconditions* must all be satisfied. When an action is applied, the world is updated in a manner specified by a set of *effects*. For example, action Pick-place(*?body*, *?region_from*, *?region_to*, *?traj*) transports *?body* from *?region_from* to *?region_to* by following a trajectory *?traj*. It has preconditions {On(*?body*, *?from*)} and effects of {¬On(*?body*, *?region_from*), On(*?body*, *?region_to*)}.

A PDDL task is a tuple $T = \langle Objects, S, G, Actions \rangle$. It is about finding a sequence of actions from set *Actions* that when applied in succession will transform the world from the initial state *S* into one in which all literals of *G* are true. *Objects* is a finite set of objects associated to the task. Let us consider the planning task of Fig. 1a. The initial state, goal state, and available actions for this scenario are

$$S_0 = \{ \text{On}(\text{body1}, \text{region1}) \} \quad (1)$$

$$G_0 = \{ \text{On}(\text{body1}, \text{region2}) \} \quad (2)$$

$$Actions_0 = \{ \text{Pick-place}(\text{?body}, \text{?from}, \text{?to}, \text{?traj}) \} \quad (3)$$

$$Objects_{ideal} = \{ \text{body1}, \text{region1}, \text{region2}, \text{traj112} \} \quad (4)$$

The object set in (4) is *ideal* in a sense that a collision-free trajectory traj112 is readily predefined. traj112 connects precisely the current pose and the target pose of body1, and it is not applicable to other scenarios where these poses are even slightly changed. Then a symbolic plan with just one member action can be found as

$$\pi = \langle \text{Pick-place}(\text{body1}, \text{region1}, \text{region2}, \text{traj112}) \rangle. \quad (5)$$

PDDLStream. From (4), one may notice the limitation of applying vanilla PDDL to robotic tasks in the sense that some of the objects, like the trajectory traj112 in (4), must be hard-coded to fit the specific scenario. PDDLStream [6] attempts to increase the universality of the system by incorporating *streams* into PDDL operators in addition to actions. Similar

TABLE I: The stream set $Streams_0$ of the transportation problem.

Stream	Description
Sample-pose(<i>?body</i> , <i>?region</i>) → <i>?pose</i>	Generate a collision-free <i>?pose</i> for <i>?body</i> on <i>?region</i> .
Plan-motion (<i>?body</i> , <i>?pose_from</i> , <i>?pose_to</i>) → <i>?traj</i>	Generate a collision-free <i>?traj</i> that transports <i>?body</i> from <i>?pose_from</i> to <i>?pose_to</i> .

to PDDL, a PDDLStream task can be represented as a tuple $T_{stream} = \langle Objects, S, G, Actions, Streams \rangle$. Streams give out new objects during planning as black-box generators of any kind. This kind of operators is crucial to a *general-purpose TAMP system* for easily integrating state-of-the-art sub-task solvers. Let us assume the streams for the transportation problem, as shown in Table I. Then, the planner can start with a set of *undemanding* objects

$$Objects_0 = \{ \text{body1}, \text{pose11}, \text{region1}, \text{region2} \} \quad (6)$$

where pose11 is the initial pose of body1 in region1, and it is easily accessed. A skeleton plan π_s composed of both actions and streams can be found as

$$\begin{aligned} & \langle \text{Sample}(\text{body1}, \text{region2}) \rightarrow \# \text{pose12}, \\ & \text{Plan-motion}(\text{body1}, \text{pose11}, \# \text{pose12}) \rightarrow \# \text{traj112}, \\ & \text{Pick-place}(\text{body1}, \text{region1}, \text{region2}, \# \text{traj112}) \rangle. \end{aligned} \quad (7)$$

where the objects generated by streams are marked by # and they demand further *bindings* to concrete values before the plan can be executed by the robot. These symbolized outputs are *optimistic* in the sense that they may not ever find their concrete counterparts under the search constraints. Thus, not all skeletons can be instantiated to concrete plans. Conversely, we assume that a concrete plan π_c feasible to the robotic task *T* is always implied by some skeleton π_s complying with the symbolic constraint.

Assumption 1: Loose symbolic constraint. The constraint imposed by symbolic planning is strictly looser than that of the real task so that the symbolic planner is not exclusive of any potentially feasible plans.

This assumption is relatively mild for most correctly defined PDDL descriptions. Through a symbolic description as (3) rules out the possibility of using actions like "Push" or "Throw" to achieve the transportation task in Fig. 1, the solution space by "Pick-place" is almost intact. The optimistic object introduced by PDDLStream is essential to the decomposition of the original manipulation planning problem into sub-problems of symbolic task planning and metric motion planning [27].

IV. TOP-K SKELETON PLANNING

Most TAMP systems satisfy their symbolic goals based on a single "best" skeleton. However, such a skeleton is usually vulnerable to the partially described environment during task planning. Let P_T be the set of all symbolic plans (possibly infinite) for a planning task *T*. The objective of top-k planning is to determine a set of *k* different plans $\{\pi_1, \pi_2, \dots, \pi_k\} = P \subseteq P_T$ with the lowest costs for a given AI planning task

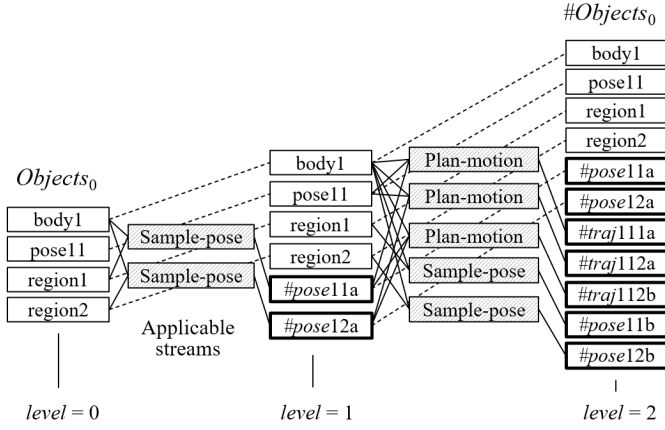


Fig. 2: A basic planning graph is used to optimistically expand the initial object set $Objects_0$ to $\#Objects_0$. The optimistic objects generated by streams are highlighted by bold boxes.

[19]. We call a top-k algorithm *sound* iff it reports only valid plans and there exists no plan $\pi' \in P_T$ while $\pi' \notin P$ that has lower cost. A top-k algorithm is *complete* iff it could find the set of all plans as required. A standard top-k planner can be described as $P = \text{TOP-K}(Objects, S, G, Actions, k)$. Compared to classical PDDL algorithm, top-k planner possesses an additional parameter $k = |P|$. We propose a top-k skeleton planner for general TAMP problems. We adopt the idea of including streams as additional operators from PDDLStream [6, 10]. A skeleton gives the sequence of operators for goal achievement, indicating when to sample for new objects by streams and when to update the environment state by actions. Searching for a set of top-k skeletons is our aim in task planning.

Skeleton planning starts with (i) optimistic enrichment of the initial object set and the initial state set such that (ii) a variety of *action plans* can be found by a top-k symbolic planner. Streams are ignored during top-k planning since their presences are not accountable to the diversity of the final plans. (iii) Next, a skeleton is recovered from each action plan by retracing all supportive streams. And finally we have top-k skeletons produced.

A. Graph expansion for optimistic object generation

Algorithm 1: OPTMS-EXPD

Input: $Objects, S, Streams, level$
 $\#Objects = \text{copy}(Objects)$
 $\#S = \text{copy}(S)$
for $i \in [1, 2, \dots, level]$ **do**
 $\#Objects, \#S =$
 NEXT-LAYER($\#Objects, S, Streams$)
return $\#Objects, \#S$

We use forward graph expansion with all streams, denoted S_0 , as operators to enrich the initial object set while limiting the level of the planning graph (see Fig. 2). The object set

in level 2 is enough to make skeleton plans like (7) possible. In the graph expansion, the first layer consists of the original objects (e.g., (6)), and the second layer is made-up of applicable streams whose preconditions are satisfied by the previous layer. Unique optimistic values are generated by the streams of the second layer, and are listed in the third layer. The expansion goes on until the maximum level is reached. This optimistic expansion is summarized in Alg. 1, where $Objects$ and $\#Objects$ denote the initial object set and the optimistically expanded set, respectively. $Streams$ are the set of all available streams in the task, e.g., Table I. As new objects are generated, the original initial set S as shown in (1) might also be expanded to $\#S$. The operation NEXT-LAYER expands the graph by one level as shown in Fig. 2. For example, after applying Alg. 1 to $Objects_0$ in (6) with $level = 2$, we get

$$\begin{aligned} \#Objects_0 = \{ & \text{body1}, \text{pose11}, \text{region1}, \text{region2}, \\ & \text{\#pose11a}, \text{\#pose12a}, \text{\#traj111a}, \\ & \text{\#traj112a}, \text{\#traj112b}, \text{\#pose11b}, \\ & \text{\#pose12b} \}. \end{aligned} \quad (8)$$

In (8), the difference between $\#traj112a$ and $\#traj112b$ is not trivial: $\#traj112a$ connects the initial pose of body1 on region1 (pose11) to an optimistic pose on region2 (\#pose12a); while $\#traj112b$ connects another optimistic pose of body1 on region1 (\#pose11a) to \#pose12a .

B. Searching top-k action plans

Here we are only interested in the diversity of the actions' arrangement. Starting from the expanded sets, $\#Objects$ and $\#S$, we formulate the top-k planning problem with only actions as PDDL operators

$$P_a = \text{TOP-K}(\#Objects, \#S, G, Actions, k) \quad (9)$$

where G and $Actions$ are with the original problem description as in (2) and (3), and $k = |P_a|$. The planning subroutine TOP-K can be any complete and sound symbolic top-k planner. Here we choose the SYM-K algorithm [19].

C. Building top-k skeletons

Now we need to recovery the top-k skeletons P_s from the action plans P_a . A skeleton plan π_s must build on only undemanding PDDL conditions, e.g., S_0 from (1) and $Objects_0$ from (6). For a action plan π_a , we retrace streams that are responsible for the optimistic objects $\#Objects_0 \setminus Objects_0$ consumed by the actions of π_a , and include them into a skeleton plan. We formalize this stream-retracing procedure as another symbolic planning problem and solve it as follows

$$\begin{aligned} \pi_s = \text{TOP-K}(& Objects, S, G_s(\pi_a, G), \\ & Actions \cup Streams, 1) \end{aligned} \quad (10)$$

$Objects, S$, and G are from the original task description. $Actions$ and $Streams$ constitute the operator set of this planning problem. Informally, by setting $k = 1$, the top-k algorithm reduces to a classical PDDL planner. To ensure that

all member actions have the same presence in π_s , as in π_a , we must add extra constraints to the goal state. Here, we make the goal state a function of π_a . Assuming $\pi_a = \langle a_1, a_2, \dots, a_n \rangle$, we have

$$G_s(\pi_a, G) = \{(a_1 \prec a_2), \dots, (a_{n-1} \prec a_n)\} \cup G, \quad (11)$$

where $(a_1 \prec a_2)$ denotes a literal asserting that a_1 must be the predecessor of a_2 .

D. The top-k skeleton planning algorithm

An overview of our proposed skeleton planning algorithm is shown in Alg. 2. The inputs of the algorithm include the original initial state S , goal state G , available *Streams* and *Actions*, and a desired number of skeletons k . The output P_s is the list of the top k skeletons, if it is found under a preset level limit *max-level* in the optimistic expansion of Alg. 1. As illustrated in Fig. 2, the size of *#Objects* ramps up quickly with increasing *level*, and consequently the complexity of the planning problem. To address this, in Alg. 2 we regulate the number of optimistic objects by progressively increasing the *level* during the searching process.

Property 1: Probabilistic completeness in skeleton planning. Under the assumption 1, given a complete top-k planner, any potentially feasible skeleton will be contained by the result set of Alg. 2 as k goes to infinity.

We choose SYM-K [19] as our planning subroutine in this study. Due to its proved completeness and soundness, the property mentioned previously is well maintained. For the simple 2-body transportation task of Fig. 1b, the robot should relocate the taller red body, for accessing and relocating the green one. Applying our proposed Alg. 2 to the task $T_{stream, 1-body} = \langle (6), (1), (2), (3), \text{Table I} \rangle$, with (10) we get a feasible skeleton as:

$$\begin{aligned} &\langle \text{Sample-pose}(\text{body2}, \text{region1}) \rightarrow \#pose21a, \\ &\text{Plan-motion}(\text{body2}, \text{pose21}, \#pose21a) \rightarrow \#traj211a, \\ &\text{Pick-place}(\text{body2}, \text{region1}, \text{region1}, \#traj211a), \\ &\text{Sample-pose}(\text{body1}, \text{region2}) \rightarrow \#pose12a, \\ &\text{Plan-motion}(\text{body1}, \text{pose11}, \#pose12a) \rightarrow \#traj112a, \\ &\text{Pick-place}(\text{body1}, \text{region1}, \text{region2}, \#traj112a) \rangle. \end{aligned} \quad (12)$$

Please refer to Appendix IX for the description of the 2-body transportation task, solved with our proposed Alg. 2.

V. TREE SEARCH IN THE EXTENDED DECISION SPACE

A skeleton π_s describes a symbolically feasible path to the goal state. Its geometric feasibility must be evaluated along with the sequential bindings of its optimistic objects to concrete values. For example, there are 4 bindings to be decided in (12). As the decisions of the bindings are causally related to each other, and they extend to large sizes as the task horizon increases, we propose using an MCTS-like approach that can systematically explore this broad decision space.

Algorithm 2: TOP-K-SKELETON

Input: $Objs, S, G, Actions, Streams, k$
for $level \in [0, 1, \dots, \text{max-level}]$ **do**
 $\#Objs, \#S =$
 OPTMS-EXPD($Objs, S, Streams, level$), see
 Alg. 1
 $P_a = \text{TOP-K}(\#Objs, \#S, G, Actions, k)$, see
 (9)
 if $|P_a| < k$ **then**
 continue for
 $P_s = \{\}$
 for $\pi_a \in P_a$ **do**
 $Operators = Actions \cup Streams$
 $\#G = G_s(\pi_a, G)$, see (11)
 $\pi_s = \text{TOP-K}(Objs, S, \#G, Operators, 1)$, see
 (10)
 $P_s \leftarrow \{\pi_s\} \cup P_s$
return P_s

TABLE II: Nodes of the binding tree model of the skeleton in (12)

Node	Member operators
decision1	Sample-pose(body2, region1) \rightarrow #pose21a
transition1	Plan-motion(body2, pose21, #pose21a) \rightarrow #traj211a Pick-place(body2, region1, region1, #traj211a)
decision2	Sample-pose(body1, region2) \rightarrow #pose12a
transition2	Plan-motion(body1, pose11, #pose12a) \rightarrow #traj112a Pick-place(body1, region1, region2, #traj112a)

A. The extended decision tree

We pose the decision over multiple skeletons as a multi-armed bandit problem, and it can be satisfactorily solved by UCB1 as shown in (14). In particular, we use UCT to make optimal sequential decisions for the binding list of each selected skeleton. In practice, not all optimistic objects of a skeleton necessarily belong to its binding list. Following [28], we can group the operators of (12) into two distinct and alternating types of nodes (see Table II and Fig. 3), the *transition* and the *decision* nodes. Operators like "Plan-motion" (with random outputs by RRT planners [23]) and "Pick-place" (with possibly positioning error—not implemented in this work) in (12) are modeled as stochastic transition systems. On the other hand, "Sample-pose" is completely depended on the task, and considers for example decision over different placement poses *pose21a* and *pose12a*, hence making it a *decision node*.

For simplicity, we pack successive transitional operators into a single transition node in Table II, e.g., "Plan-motion" and "Pick-place" belong to the same transition node. Finally, we can formulate the skeleton-selection and the binding search with a single model, based on the observation that skeleton-selection is just an extended decision node at the root of a decision tree. As a result, an extended decision tree can be built, as shown Fig. 3.

B. Binding search in the extended decision tree

Starting from the extended root, a robot must make sequential decisions along the tree until a terminal state is

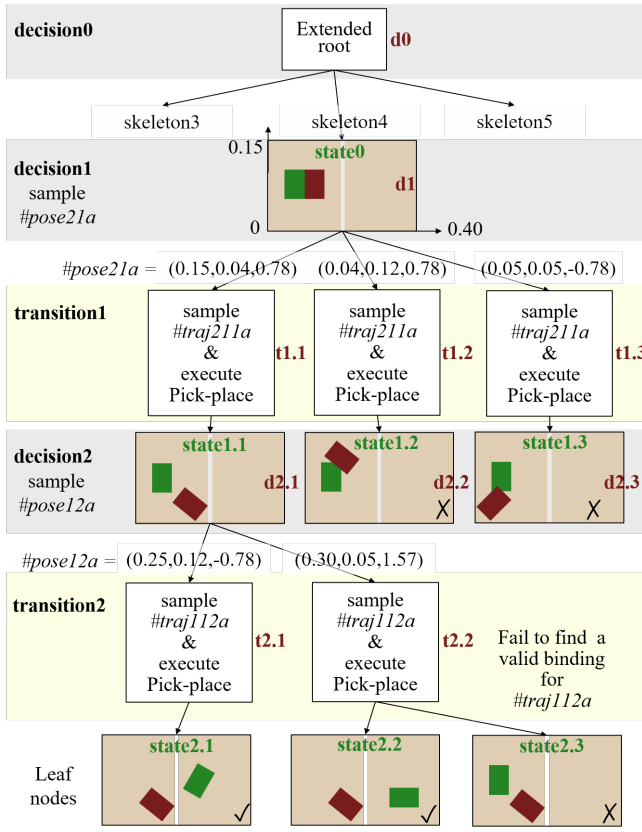


Fig. 3: An example of an extended decision tree for solving the 2-body transportation task of Fig. 1b

encountered. A *terminal state* indicates that the state of the current node is infeasible to the task, and binding search must stop here (e.g., state1.2 and state1.3 in Fig. 3). Then it will receive a reward $r \in \mathbb{R}$. The robot’s objective is to find a sequence of decisions with a planning horizon H_i that maximizes the final reward. $H_i = 1 + \text{depth}_i$ where depth_i is the number of decision nodes inside the selected skeleton $\pi_{s,i}$. In our study, we use a reward function defined as

$$r = 0.1 \left(\frac{\text{depth}_{\text{end}}}{\text{depth}_i} + \frac{1}{\text{motionCost}_{\text{end}}} \right) + r_{\text{success}} \quad (13)$$

where $\text{depth}_{\text{end}}$ is the depth in the decision tree in which the current node is terminated, and $\text{motionCost}_{\text{end}}$ is proportional to the swept volume of the robot from its initial state to the terminal state. The first term in (13) is a normalized depth that encourages the robot to avoid branches where bindings have already failed earlier. The second term makes the robot prefer branches with motions that have less occupation in the workspace. For the third term, $r_{\text{success}} = 1$ when all bindings are successfully found, otherwise $r_{\text{success}} = 0$. This reward design is effective for solving an array of robot manipulation problems, as we show in Sec. VI, and it can be specialized for better performance in specific tasks.

By now, we have a classical finite-horizon stochastic optimal search problem, and it can be described as a Markov Decision Process (MDP). With the UCT formulation, episodic MDP is repeated during the search loop, and information from the

previous episodes is used for reaching optimal decisions in the subsequent episodes. The information, in this case, refers to the value V and the visit number M of a tree node.

Since UCT is originally proposed for solving planning with discrete decision spaces, and we have continuous bindings to decide on (e.g., $\#pose12a$ in Fig. 3), we employ a UCT variant with progressive widening (PW) techniques [29, 28, 30]. The basic idea is to limit the number of visits for existing nodes artificially. When the value of the existing nodes is estimated sufficiently well, new nodes will be created to explore the unreached regions of the decision spaces. As with UCT, the paramount task of PW-UCT is to consistently estimate each node’s value, despite of stochastic transitions. Within a selected tree branch of π_s , we denote $p(z'|z, u)$ the probability of having a decision node z' after taking a decision u at decision node z . By Bellman equation [31], the optimal value $V^*(w)$ of a transition node $w = (z, u)$ is

$$V^*(w) = \begin{cases} r & \text{if } w \text{ is terminated,} \\ \int_{z'} V^*(z') dp(z'|z, u) & \text{else.} \end{cases}$$

Backpropagating to its parent node, the optimal value $V^*(z)$ of the decision node z is

$$V^*(z) = \begin{cases} r & \text{if } z \text{ is terminated,} \\ \sup_u V^*(z, u) & \text{else.} \end{cases}$$

Similar to the average reward in (15), $V^*(w)$ and $V^*(z)$ are fundamental to the UCB criterion for optimal decision making. Thus, consistent estimation of these values is highly demanded. Assume $\hat{V}(z)$, $\hat{V}(w)$ as the empirical average values of z , w , and $M(z)$, $M(w)$ as their total visit numbers. According to [28], we have $\hat{V}(z) \rightarrow V^*(z)$ when $M(z)$ goes infinite, if we comply with a PW-LAW(*node*) (see in the Appendix, Alg. 8 for details) which decides whether to explore a new decision at z , or whether to start a new simulation thread at w . The original criterion, however, assumes that the new decisions at z are always available, while it is not the case when decisions at a node are discrete and enumerable. To counteract this restriction, we define a new PW law with Alg. 3, that supports streams with both continuous and discrete outputs for more versatile robotic applications.

The argument $\text{False} = \text{EXPAND-TEST}(\text{node})$ means that new edges cannot be created from *node* at the time. In this case, an existing edge connecting to an established child of *node* must be selected. For *decision nodes*, we use the UCB-SELECT(*node*) strategy to select the child of *node* with the maximum UCB score (see (14)). For *transition nodes*, the strategy of LEAST-SELECT(*node*) is used to simply select the least-visited child of *node*. The overall child selection strategy is in Alg. 4.

If $\text{True} = \text{EXPAND-TEST}(\text{node})$, new edges leading from *node* to a new child node must be created. For *decision nodes*, we use the NEW-DECISION(*node*) strategy to sample a new decision and create the resultant child node. With this strategy, *node* with discrete stream outputs will randomly select an unvisited decision; *node* with continuous stream outputs will

Algorithm 3: EXPAND-TEST

```

Input: node
if node is a decision node then
  |  $s = \text{streamFromNode}(\text{node})$ 
  | if  $s.\text{output}$  is continuous then
  | | return PW-LAW(node)
  | else
  | | if  $s.\text{outputSpace} \subseteq \{z.\text{decisionHistory}\}$  then
  | | | return False
  | | else
  | | | return True
else
  | return PW-LAW(node)

```

Algorithm 4: CHILD-SELECT

```

Input: node
if node is a decision node then
  |  $\text{child\_node} = \text{UCB-SELECT}(\text{node})$ 
else
  |  $\text{child\_node} = \text{LEAST-SELECT}(\text{node})$ 
return child_node

```

use Voronoi sampling to choose the next concrete binding for rapid exploration of the decision space. For the *transition* node, we define a subroutine called NEW-TRANSITION(*node*) that evaluates randomly the streams of (*node*). These randomly generated bindings then direct the environment to a new state on which a new child node is built. At last, we can summarize our extended tree search algorithm in Alg. 6. Its inputs include the top-k skeleton set P_s generated by Alg. 2 and a user-defined time budget t_{ts} . The output of Alg. 6 is a single concrete plan π_c that is optimized under given t_{ts} . On RECEIVE-VISIT(*node*), *node* will increase its visit number by 1. Meanwhile, all actions ahead of *node* in the skeleton will be effectuated to update the environment to which state *node* is initially built on. For example in Fig. 3, RECEIVE-VISIT(d1) will reset the environment to state0, and RECEIVE-VISIT(d2.1) will set it to state1. By complying with the laws of node selection and node expansion of Alg. 4 and Alg. 3, a global convergence of the output π_c to the optimal plan is guaranteed. We refer to [28] for the detailed proof.

Property 2: Probabilistic completeness in the extended tree search. Alg. 6 is structured in line with the PW-UCT framework, and it retains all the convergence property. The optimal concrete plan within the extended decision space (implied by P_s) can be found after t_{ts} goes infinite.

C. The eTAMP algorithm

A serial combination of Alg. 2 and Alg. 6 gives out the overall eTAMP algorithm, as summarized in Alg. 7. It takes as input a standard PDDLStream task $T_{stream} = \langle \text{Objects}, S, G, \text{Actions}, \text{Streams} \rangle$, and two hyper-parameters: k and t_b , allocating computational

Algorithm 5: NEW-CHILD

```

Input: node
if node is a decision node then
  |  $\text{new\_node} = \text{NEW-DECISION}(\text{node})$ 
else
  |  $\text{new\_node} = \text{NEW-TRANSITION}(\text{node})$ 
  |  $\text{node.addChild}(\text{new\_node})$ 
return new_node

```

Algorithm 6: EXTENDED-TREE-SEARCH

```

Input:  $P_s, t_{ts}$ 
 $\text{extened\_root} = \text{buildExtendedRoot}(P_s)$ 
 $\text{node} \leftarrow \text{extened\_root}$ 
while  $\text{timeCost}() < t_{ts}$  do
  | while node is not terminated do
  | | RECEIVE-VISIT(node)
  | | if EXPAND-TEST(node) then
  | | |  $\text{node} \leftarrow \text{NEW-CHILD}(\text{node})$ , see Alg. 5
  | | | else
  | | | |  $\text{node} \leftarrow \text{CHILD-SELECT}(\text{node})$ , see Alg. 4
  | | | |  $\text{backupRewardFrom}(\text{node})$ 
  | |  $\text{node} \leftarrow \text{extened\_root}$ 
  |  $\pi_c = \text{highestValueBranchFrom}(\text{extened\_root})$ 
return  $\pi_c$ 

```

Algorithm 7: eTAMP

```

Input:  $T_{stream}, k, t_b$ 
 $P_s = \text{TOP-K-SKELETON}(T_{stream}, k)$ , see Alg. 2
 $t_{ts} = t_b - \text{timeCost}()$ 
 $\pi_c = \text{EXTENDED-TREE-SEARCH}(P_s, t_{ts})$ , see Alg. 6
return  $\pi_c$ 

```

resources to the planner. Its dependencies include a set of black-box generators for streams, and a robotic simulator.

VI. EMPIRICAL EVALUATION

We empirically evaluate the proposed eTAMP algorithm in three multi-stage robot manipulation tasks: transportation, cooking, and regrasping. None of them can be solved by a whole-piece motion planner, or a standalone AI planner. The Adaptive algorithm from [6] represents the best performance of existing PDDLStream methods, and it serves as a baseline in these evaluation tasks. The two general-purpose TAMP algorithms, adaptive PDDLStream, and eTAMP, share one internal simulator that is implemented with PyBullet [32] for hosting the environment state. Both planners are terminated after a 700-second timeout for each of the three tasks. For eTAMP we set $k = 50$ (please see Appendix X-A for details), and it is shown enough for the considered tasks. The performance of each algorithm is evaluated over 100 instances of each task. Whenever a feasible concrete plan is found, the

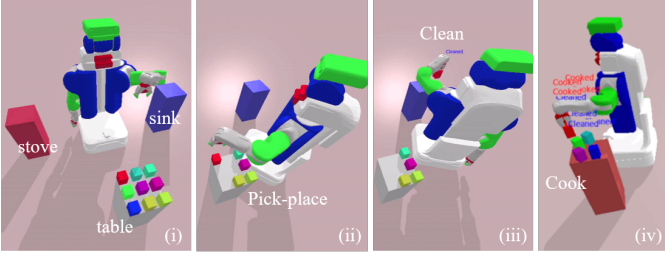


Fig. 4: The cooking task: Given an initial number of bodies to be cooked, the mobile manipulator should cook by first placing the body on the sink for cleaning, and then place it on the stove for washing.

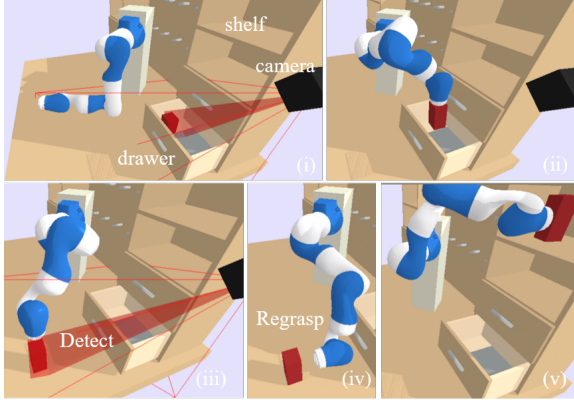


Fig. 5: The regrasping task: The only way the robot could move the cuboid body from the drawer to the shelf is by regrasping it with a different direction after taking it from the drawer.

algorithm is stopped and the computation time is calculated. These diverse instances are generated by randomly initializing the initial geometric state. It is noteworthy that both algorithms employ the same set of random stream generators for decision nodes, which have zero built-in heuristics.

A. The transportation task

This task comes directly from the motivation example of Fig. 1. For the 1-body scenario, Adaptive PDDLStream and eTAMP can solve the problem respectively in **0.44 s** and **3.94 s** on average. The larger time cost of eTAMP is due to the extra effort of its top- k planner in finding all the k alternatives, which in this case are somewhat “unnecessary”. A trivial plan such as plan1 in Table III (see Appendix) is enough in this case. When more than one body is involved, the problem becomes more challenging since the symbolic planners at high hierarchies are normally unaware of the detailed geometric constraints, as imposed by the taller red body in Fig. 1b. With the help of diverse backup plans such as plan4 and plan5 in Table III (see Appendix), eTAMP solves the 2-body problem in **11.95 s** on average. However, Adaptive PDDLStream is unable to find a feasible plan within the time budget of 700s. To further evaluate the algorithms, we propose a 3-body scenario as shown in Fig. 8 (see Appendix), where two bodies must be relocated before the target one can be reached. eTAMP solves this harder problem in **157.70 s** while Adaptive PDDLStream still fails to give a solution.

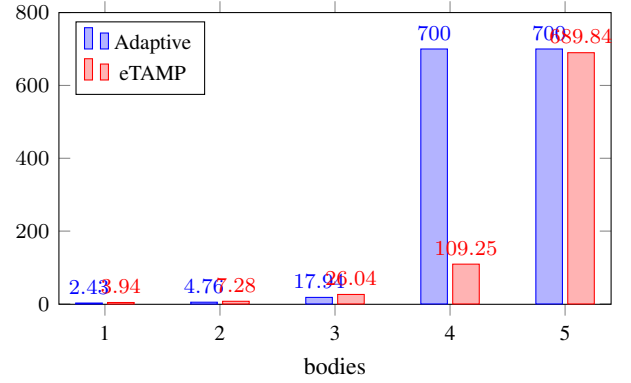


Fig. 6: Average planning cost (seconds) of Adaptive PDDLStream and eTAMP in the cooking task. A time cost of 700 means none solutions are found within the time budget.

B. The cooking task

This task evaluates the TAMP algorithms’ scalability to long-horizon manipulation and the capability to manipulate and move in narrow feasible spaces. As shown in Fig. 4, this task aims to transport a given number of bodies initially placed on the table to the stove for cooking. Before cooking, a body must be once placed on the sink for washing. The cooking task features long-horizon robot manipulation since it has several bodies to be fetched, and each body fetching and placing demands multiple steps for successful completion. For example, a task instance with 5 bodies involved requires at least 10 free-hand movements plus 10 hold-body movements. A realistic execution of such a plan on real robots can take several minutes.

The main difficulty of this task lies in the tight stove region, where several bodies need to be placed. Therefore, the decisions regarding the body pose on the stove are critical to the task’s success. As both Adaptive PDDLStream and eTAMP are uninformed about this potential congestion beforehand, they must identify this constraint through trial and error. During binding search, the consistent value estimation of each decision is critical for this delayed-reward case. Fig. 6 shows the time consumption of Adaptive PDDLStream and eTAMP in solving the cooking task. With problems with fewer bodies, eTAMP costs slightly more time than Adaptive. On larger numbers of bodies, eTAMP outperforms Adaptive PDDLStream by using optimal tree search, especially when the feasible space gets tighter (see Fig. 4 (iv)).

C. The regrasping task

In this task, the robot should transport a cuboid body from the drawer to the shelf, where it should still be placed upright. To realize a real-world setting, we consider a fixed camera that detects the pose of the object. Therefore, the robot has to query the pose detector for continuing its manipulation task. The robot can choose between 5 grasping directions to the body: along the normal vectors of the top surface and four side surfaces. The cuboid body at its initial pose is limited to top grasping by the drawer and the neighbor body, while it must be grasped from the side when being placed on the shelf, as depicted in Fig. 5. This task is difficult for skeleton

planning since a regrasping behavior must be composed by planners based on only elemental operators (please see examples in Table IV in Appendix). Otherwise, the problem cannot be solved. Moreover, this task is geometrically challenging. Even if a correct skeleton is given, the planner must search the hybrid decision space (discrete grasping directions and continuous body poses) for feasible bindings. The average time cost of eTAMP for solving this task is **235.63 s**. In comparison, Adaptive PDDLStream is unable to find any solution within the time budget.

Remarks: Our empirical evaluation shows the effectiveness of the proposed eTAMP algorithm in solving challenging, multi-stage manipulation tasks. Whereas the most competitive baseline in the literature fails to scale to increasing numbers of decision steps, our algorithm trades off slightly higher planning time in simple scenarios for high effectiveness when multi-object and multiple actions are in place. The proposed seamless combination of symbolic top-k planning with streams for searching alternative skeleton plans, with the optimality of PW-UCT, leads to a powerful algorithm that can handle the combinatorial complexity of long-horizon manipulation tasks.

VII. CONCLUSION

We propose eTAMP as a general-purpose planner of robot manipulation tasks with long horizons that demand symbolic sequencing of operators and binding search of motion parameters under geometric constraints. eTAMP addresses the difficulty of incomplete domain in task planning by using symbolic top-k planning for diverse backup skeletons. It integrates a uniform tree search method for the extended decision space based on UCB and PW that allow global convergence to optimal plans, in spite of the stochastic transition dynamics during planning. The empirical results reveal that our approach outperforms the existing state-of-the-art PDDLStream algorithm, especially in problems where alternative skeletons are indispensable. We attribute the capability of eTAMP for solving long-horizon tasks to the proposed hierarchical planner structure over actions and skeletons, and the scalability of UCT to large decision sequences (empirically proved in [33]). In future work, we will explore a more informative sampling method for stream generators to improve efficiency in binding search.

REFERENCES

- [1] L. P. Kaelbling and T. Lozano-Pérez, “Hierarchical task and motion planning in the now,” in *2011 IEEE International Conference on Robotics and Automation*, pp. 1470–1477, IEEE, 2011.
- [2] S. Srivastava, E. Fang, L. Riano, R. Chitnis, S. Russell, and P. Abbeel, “Combined task and motion planning through an extensible planner-independent interface layer,” in *2014 IEEE international conference on robotics and automation (ICRA)*, pp. 639–646, IEEE, 2014.
- [3] C. Weber and D. Bryce, “Planning and acting in incomplete domains,” in *Proceedings of the International Conference on Automated Planning and Scheduling*, vol. 21, 2011.
- [4] H. H. Zhuo, T. A. Nguyen, and S. Kambhampati, “Refining Incomplete Planning Domain Models Through Plan Traces,” in *IJCAI*, pp. 2451–2458, 2013.
- [5] N. T. Dantam, Z. K. Kingston, S. Chaudhuri, and L. E. Kavraki, “Incremental Task and Motion Planning: A Constraint-Based Approach,” in *Robotics: Science and systems*, vol. 12, p. 00052, Ann Arbor, MI, USA, 2016.
- [6] C. R. Garrett, T. Lozano-Pérez, and L. P. Kaelbling, “PDDLStream: Integrating symbolic planners and black-box samplers via optimistic adaptive planning,” in *Proceedings of the International Conference on Automated Planning and Scheduling*, vol. 30, pp. 440–448, 2020.
- [7] C. R. Garrett, R. Chitnis, R. Holladay, B. Kim, T. Silver, L. P. Kaelbling, and T. Lozano-Pérez, “Integrated task and motion planning,” *arXiv preprint arXiv:2010.01083*, 2020.
- [8] T. Nguyen and S. Kambhampati, “A heuristic approach to planning with incomplete strips action models,” in *Proceedings of the International Conference on Automated Planning and Scheduling*, vol. 24, 2014.
- [9] M. Katz, S. Sohrabi, O. Udrea, and D. Winterer, “A novel iterative approach to top-k planning,” in *Proceedings of the International Conference on Automated Planning and Scheduling*, vol. 28, 2018.
- [10] C. R. Garrett, T. Lozano-Pérez, and L. P. Kaelbling, “Stripstream: Integrating symbolic planners and blackbox samplers,” *arXiv preprint arXiv:1802.08705*, 2018.
- [11] N. Shah, D. K. Vasudevan, K. Kumar, P. Kamojihala, and S. Srivastava, “Anytime integrated task and motion policies for stochastic environments,” in *2020 IEEE International Conference on Robotics and Automation (ICRA)*, pp. 9285–9291, IEEE, 2020.
- [12] M. Toussaint, “Logic-Geometric Programming: An Optimization-Based Approach to Combined Task and Motion Planning,” in *IJCAI*, pp. 1930–1936, 2015.
- [13] Z. Kingston, A. M. Wells, M. Moll, and L. E. Kavraki, “Informing multi-modal planning with synergistic discrete leads,” in *2020 IEEE International Conference on Robotics and Automation (ICRA)*, pp. 3199–3205, IEEE, 2020.
- [14] D. McDermott, M. Ghallab, A. Howe, C. Knoblock, A. Ram, M. Veloso, D. Weld, and D. Wilkins, “PDDL—the planning domain definition language,” 1998.
- [15] C. Dornhege, P. Eyerich, T. Keller, S. Trüg, M. Brenner, and B. Nebel, “Semantic attachments for domain-independent planning systems,” in *Towards service robots for everyday environments*, pp. 99–115, Springer, 2012.
- [16] C. R. Garrett, T. Lozano-Pérez, and L. P. Kaelbling, “Sampling-based methods for factored task and motion planning,” *The International Journal of Robotics Research*, vol. 37, no. 13-14, pp. 1796–1825, 2018.
- [17] M. Helmert, “The fast downward planning system,” *Journal of Artificial Intelligence Research*, vol. 26, pp. 191–

246, 2006.

- [18] A. Torralba, V. Alcázar, D. Borrajo, P. Kissmann, and S. Edelkamp, “SymBA*: A symbolic bidirectional A* planner,” in *International Planning Competition*, pp. 105–108, 2014.
- [19] D. Speck, R. Mattmüller, and B. Nebel, “Symbolic top-k planning,” in *Proceedings of the AAAI Conference on Artificial Intelligence*, vol. 34, pp. 9967–9974, 2020.
- [20] L. Kocsis and C. Szepesvári, “Bandit based monte-carlo planning,” in *European conference on machine learning*, pp. 282–293, Springer, 2006.
- [21] P.-A. Coquelin and R. Munos, “Bandit algorithms for tree search,” *arXiv preprint cs/0703062*, 2007.
- [22] B. Kim, K. Lee, S. Lim, L. Kaelbling, and T. Lozano-Pérez, “Monte Carlo tree search in continuous spaces using Voronoi optimistic optimization with regret bounds,” in *Proceedings of the AAAI Conference on Artificial Intelligence*, vol. 34, pp. 9916–9924, 2020.
- [23] S. M. LaValle *et al.*, “Rapidly-exploring random trees: A new tool for path planning,” 1998.
- [24] S. M. LaValle and J. J. Kuffner Jr, “Randomized kino-dynamic planning,” *The international journal of robotics research*, vol. 20, no. 5, pp. 378–400, 2001.
- [25] J. Hoffmann and B. Nebel, “The FF planning system: Fast plan generation through heuristic search,” *Journal of Artificial Intelligence Research*, vol. 14, pp. 253–302, 2001.
- [26] M. Fox and D. Long, “PDDL+: Modeling continuous time dependent effects,” in *Proceedings of the 3rd International NASA Workshop on Planning and Scheduling for Space*, vol. 4, p. 34, 2002.
- [27] C. Dellin and S. Srinivasa, “A unifying formalism for shortest path problems with expensive edge evaluations via lazy best-first search over paths with edge selectors,” in *Proceedings of the International Conference on Automated Planning and Scheduling*, vol. 26, 2016.
- [28] D. Auger, A. Couetoux, and O. Teytaud, “Continuous upper confidence trees with polynomial exploration-consistency,” in *Joint European Conference on Machine Learning and Knowledge Discovery in Databases*, pp. 194–209, Springer, 2013.
- [29] R. Coulom, ““elo ratings” of move patterns in the game of go,” *ICGA journal*, vol. 30, no. 4, pp. 198–208, 2007.
- [30] G. M. J. Chaslot, M. H. Winands, H. J. V. D. HERIK, J. W. Uiterwijk, and B. Bouzy, “Progressive strategies for Monte-Carlo tree search,” *New Mathematics and Natural Computation*, vol. 4, no. 03, pp. 343–357, 2008.
- [31] R. Bellman, “Dynamic programming,” *Science*, vol. 153, no. 3731, pp. 34–37, 1966.
- [32] E. Coumans and Y. Bai, “Pybullet, a python module for physics simulation for games, robotics and machine learning,” URL <http://pybullet.org>.
- [33] D. Silver, A. Huang, C. J. Maddison, A. Guez, L. Sifre, G. Van Den Driessche, J. Schrittwieser, I. Antonoglou, V. Panneershelvam, M. Lanctot, *et al.*, “Mastering the game of Go with deep neural networks and tree search,”

nature, vol. 529, no. 7587, pp. 484–489, 2016.

- [34] L. Kocsis, C. Szepesvári, and J. Willemson, “Improved monte-carlo search,” *Univ. Tartu, Estonia, Tech. Rep*, vol. 1, 2006.
- [35] P. Auer, N. Cesa-Bianchi, and P. Fischer, “Finite-time analysis of the multiarmed bandit problem,” *Machine learning*, vol. 47, no. 2, pp. 235–256, 2002.

APPENDIX

VIII. ADDITIONAL METHODOLOGICAL BACKGROUND

We will provide an overview of Monte Carlo Tree Search method. Next, we discuss the UCB algorithm and subsequently an extension of UCB to the UCT algorithm.

1) *Monte-Carlo Tree Search*: MCTS combines tree search with Monte-Carlo sampling to build a tree, in which the states and decisions are nodes and edges, respectively, with the purpose of optimal computing decisions. The MCTS algorithm consists of a loop of four steps:

- **Selection**: starting from the root node, we interleave decision selection and sampling of the next state (tree node) until a leaf node is reached
- **Expansion**: add a new edge (decision) to the leaf node and sample a next state (new leaf node)
- **Simulation**: rollout from the reached state to the end of the episode using random decisions or a heuristic method
- **Backup**: update the nodes backwards along the trajectory starting from the last reached state of the episode till the root node according to the collected rewards

2) *Upper Confidence Bound for Trees*: In this work, we consider UCT (Upper Confidence bounds for Trees) [34], an extension of the well-known UCB1 [35] multi-armed bandit algorithm. UCB1 chooses the arm (decision u) using

$$u = \arg \max_{i \in \{1 \dots K\}} \bar{X}_{i, M_i(n-1)} + C \sqrt{\frac{\log n}{M_i(n-1)}}. \quad (14)$$

where $M_i(n) = \sum_{t=1}^n \mathbf{1}\{t = i\}$ is the number of times arm i is played up to time n . $\bar{X}_{i, M_i(n-1)}$ denotes the average reward of arm i up to time $n-1$ and $C = \sqrt{2}$ is an exploration constant. In UCT, each node is a separate bandit, where the arms correspond to the actions, and the payoff is the reward of the episodes starting from them. In the backup phase, the value is backed up recursively from the leaf node to the root as

$$\bar{X}_n = \sum_{i=1}^K \left(\frac{M_i(n)}{n} \right) \bar{X}_{i, M_i(n)}. \quad (15)$$

[34] proved that UCT converges in the limit to the optimal policy.

3) *The Progressive Widening Law for UCT*: We summarize the PW law for expansion of continuous decision nodes in UCT as follows.

where index α is the corresponding constant for balancing exploration with exploitation [28].

Algorithm 8: PW-LAW

Input: *node*
if *node* is a decision node **then**
 | **return** $\lfloor M(z)^\alpha \rfloor > \lfloor (M(z) - 1)^\alpha \rfloor$
else
 | **return** $\lfloor M(w)^\alpha \rfloor \neq \lfloor (M(w) - 1)^\alpha \rfloor$

TABLE III: Example top-k symbolic plans

Action plan	Member actions in sequence
plan1	Pick-place(body1,region1,region2,#traj112a)
plan2	Pick-place(body1,region1,region1,#traj111a) Pick-place(body1,region1,region2,#traj112b)
plan3	Pick-place(body1,region1,region2,#traj112a) Pick-place(body2,region1,region2,#traj212a)
plan4	Pick-place(body2,region1,region1,#traj211a) Pick-place(body1,region1,region2,#traj112a)
plan5	Pick-place(body2,region1,region2,#traj212a) Pick-place(body1,region1,region2,#traj112a)
...	...

Fig. 7: State evolution of the 2-body transportation scenario when different action plans are applied. The goal is to move the green body (body1) from the left region (region1) to the right one (region2). The manipulation sequence of Fig. 1b is consistent with plan4.

IX. 2-BODY TRANSPORTATION TOY-EXAMPLE

Here, we presented a solution of the 2-body transportation task, of Fig. 1b using Alg. 2. Compared to the 1-body scenario $T_{stream,1-body} = \langle (8), (1), (2), (3), \text{Table I} \rangle$, the PDDLStream description of this problem is only different in terms of the initial state and the initial object set:

$$S_1 = \{ \text{On}(\text{body1}, \text{region1}), \text{On}(\text{body2}, \text{region1}) \} \quad (16)$$

$$\text{Objects}_1 = \{ \text{body1}, \text{pose11}, \text{body2}, \text{pose21}, \text{region1}, \text{region2} \}. \quad (17)$$

The problem is now described as $T_{stream,2-body} = \langle (17), (16), (2), (3), \text{Table I} \rangle$. Example outputs from the top-k action planner of (9) are summarized in Table III, and their respective state evolution as indicated by these action plans are depicted in Fig. 7

Although all plans can reach the goal state in a symbolic sense, they choose different strategies for moving the bodies. Most TAMP planners have no problem finding the first plan. However, when this strategy is later found infeasible due to the taller red body's geometric constraints (body2), these planners tend to get stuck. Our planner can bypass the dead-end with

TABLE IV: An example of feasible skeleton plan to the regrasping task found by eTAMP. The member operators are grouped into macro behaviors.

Behavior	Member operators
Approach and pick	Detect-body(\cdot, \cdot, \cdot)
	Sample-grasp-direction(\cdot, \cdot) $\rightarrow \#$
	Inverse-kinematics($\cdot, \cdot, \#$) $\rightarrow \#, \#$
	Plan-free-motion($\cdot, \#$) $\rightarrow \#$
	Move-free($\cdot, \#, \#$) Pick($\cdot, \cdot, \#, \#, \#$)
Carry and place	Sample-place(\cdot, \cdot) $\rightarrow \#$
	Inverse-kinematics($\cdot, \cdot, \#$) $\rightarrow \#, \#$
	Plan-holding-motion($\#, \#, \cdot, \#$) $\rightarrow \#$
	Move-holding($\#, \#, \cdot, \#, \#$) Place($\cdot, \#, \cdot, \#, \#, \#$)
Regrasp	Detect-body($\cdot, \#, \cdot$)
	Sample-grasp-direction($\cdot, \#$) $\rightarrow \#$
	Inverse-kinematics($\cdot, \#, \#$) $\rightarrow \#, \#$
	Plan-free-motion($\#, \#$) $\rightarrow \#$
	Move-free($\#, \#, \#$) Pick($\cdot, \#, \#, \#, \#$)
Carry and place	Sample-place(\cdot, \cdot) $\rightarrow \#$
	Inverse-kinematics($\cdot, \#, \#$) $\rightarrow \#, \#$
	Plan-holding-motion($\#, \#, \cdot, \#$) $\rightarrow \#$
	Move-holding($\#, \#, \#, \#, \#$) Place($\cdot, \#, \cdot, \#, \#, \#$)
Back to home	Plan-free-motion($\#, \cdot$) $\rightarrow \#$
	Move-free($\#, \cdot, \#$)

all its alternative symbolic plans. Obviously, not all candidate plans will contribute to the solution. For example, plan2 and plan3 still fail to find the plan for grasping the green body. However, if there exist any feasible solutions to the problem, Alg. 2 is bound to find them, like plan4 and plan5.

Action plans as shown in Table III are further processed by (10) and their corresponding skeletons are generated, e.g. after retracing all streams for plan4, we get its successor skeleton4 (same solution as in (12) but mentioned again for convenience):

$$\begin{aligned} &\langle \text{Sample-pose}(\text{body2}, \text{region1}) \rightarrow \# \text{pose21a}, \\ &\text{Plan-motion}(\text{body2}, \text{pose21}, \# \text{pose21a}) \rightarrow \# \text{traj211a}, \\ &\text{Pick-place}(\text{body2}, \text{region1}, \text{region1}, \# \text{traj211a}), \\ &\text{Sample-pose}(\text{body1}, \text{region2}) \rightarrow \# \text{pose12a}, \\ &\text{Plan-motion}(\text{body1}, \text{pose11}, \# \text{pose12a}) \rightarrow \# \text{traj112a}, \\ &\text{Pick-place}(\text{body1}, \text{region1}, \text{region2}, \# \text{traj112a}) \rangle. \end{aligned} \quad (18)$$

From (18), one can see a production-consumption-like dependency between streams and actions, where producers like "Sample-pose" and "Plan-motion" generate optimistic objects. These objects are then consumed by downstream actions or other streams. The environment state changes whenever an action is encountered.

X. EXPERIMENT DETAILS

Details of hyperparameter setting for algorithms and experimental results are given here. Both TAMP algorithms involved in Sec. VI are implemented on a PC with a 3.5-GHz CPU and 16-GB RAM. Across the experiments, both algorithms stayed constant.

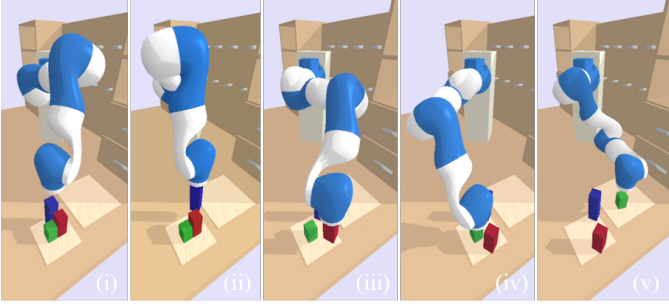


Fig. 8: The 3-body transportation task. To reach the green body, taller bodies must be relocated by the robot at first.

A. Hyperparameters

For eTAMP, we had hyperparameters as $t_b = 700s$ and $k = 50$. In general, it is advisable to have a large k value, since if k is too small, a feasible skeleton may not be found and eTAMP will return failure on timeout. On the other hand, if k is excessively large, the TOP-K algorithm will spend a lot of time on searching for unnecessary alternate skeletons.

B. The planning environment of the 3-body transpiration task

The initial state of the task is shown in Fig. 8(i) and it is an extension of the scenarios in Fig. 1. A feasible concrete plan generated by eTAMP is displayed by the subplots of Fig. 8.

C. An example skeleton for the regrasping task

As shown in Table IV, a skeleton comprises interleaved streams (operators with " \rightarrow ") and actions. Where "." and "#" are the placeholders for the original objects and the optimistic objects respectively. These symbolic operators can be further grouped by macro behaviors for a better understanding of how a long-horizon task can be solved by eTAMP.